18th International Conference on Space Operations, Montreal, Canada, 26 - 30 May 2025.

SpaceOps-2025, ID # 134

THERMAL DESIGN AND ANALYSIS OF BAHRAIN'S IN-HOUSE DEVELOPED PAYLOAD IN SUN-SYNCHRONOUS ORBIT

Yaqoob Alqassab[a]*, Yusuf Alqattan[b], Ashraf Khater[c], Muneera Almalki[d]

[a] *National Space Science Agency (NSSA), Kingdom of Bahrain, yagoob.khalid@nssa.gov.bh*
[b] *National Space Science Agency (NSSA), Kingdom of Bahrain, yusuf.alqattan@nssa.gov.bh*
[c] *National Space Science Agency (NSSA), Kingdom of Bahrain, ashraf.khater@nssa.gov.bh*
[d] *National Space Science Agency (NSSA), Kingdom of Bahrain, muneera.almalki@nssa.gov.bh*
* Corresponding Author

Abstract

Since their inception in 1999, CubeSats have evolved into a global phenomenon, revolutionizing space missions with their compact size and advanced technological capabilities. As these missions grow in complexity and incorporate an increasing number of satellite components, it becomes critical to assess how spacecraft withstand the extreme thermal cycles encountered in space. Accurate thermal simulations are essential for ensuring the survivability and operational integrity of satellites under these conditions. This paper presents a comprehensive thermal analysis and testing results of the AlMunther satellite payload, developed by engineers at Bahrain's National Space Science Agency (NSSA). The payload is destined to be onboard a 3U CubeSat, designed to orbit in a Sun Synchronous Low Earth Orbit (LEO). Notably, the AlMunther payload incorporates commercial off-the-shelf components that have not been specifically qualified for space use, underscoring the necessity for meticulous thermal evaluation. To this end, a detailed thermal model of the AlMunther payload was constructed and examined using the Finite Element Analysis (FEA) methodology. The analysis encompassed three principal scenarios: worst-case hot steady state, worst-case cold steady state, and transient states. The simulations confirmed that all electronic components of the AlMunther payload remained within their acceptable temperature ranges throughout the various modeled conditions. Following the simulation, operational and non-operational thermal testing using a thermal ambient machine was conducted to validate the analysis results. This crucial step ensured that the payload could indeed withstand the harsh thermal environment of space. These findings enable the design of a tailored thermal control system, ensuring the AlMunther payload—and, by extension, the CubeSat housing it—can withstand the harsh thermal environment of space.
Keywords: AlMunther, Thermal Analysis, Transient Analysis, CubeSat, FEA Simulation

1. Introduction

Thermal management is a fundamental aspect of satellite design, particularly for small spacecraft such as CubeSats operating in Low Earth Orbit (LEO). Due to their compact size, limited thermal mass, and constrained surface area, CubeSats are highly susceptible to extreme temperature fluctuations during orbital transitions between sunlight and eclipse phases. These thermal cycles, if not carefully mitigated, can lead to component degradation, performance instability, or even mission failure [1], [2].

CubeSats typically lack the advanced thermal control systems seen in larger spacecraft, relying instead on passive thermal strategies such as surface coatings, thermal isolation, or simple radiators [3]. This limitation increases the importance of accurate thermal analysis, especially for payloads incorporating commercial off-the-shelf (COTS) components that are not space-qualified. Such components often lack data on their behavior under vacuum, radiation exposure, or extended thermal cycling, making thorough ground-based thermal simulations and testing indispensable [4].

The AlMunther payload, developed by Bahrain's National Space Science Agency (NSSA), is integrated within a 3U CubeSat platform and is intended for deployment in a Sun-Synchronous Orbit (SSO) at approximately 550 km altitude. The payload includes imaging and processing units composed entirely of COTS components, highlighting the need for comprehensive thermal evaluation to ensure mission success.

This paper presents the thermal design and analysis of the AlMunther payload using both steady-state and transient thermal simulations based on Finite Element Analysis (FEA) techniques. The study encompasses worst-case hot and cold conditions that simulate the full range of orbital environmental extremes, including the effects of solar flux, Earth infrared (IR) radiation, and Earth albedo. The output of these simulations provides critical insights into temperature distributions across payload components and guides the development of a tailored thermal control strategy.

To ensure the validity and reproducibility of the results, the methodology incorporates several best practices in thermal modeling: a reduced CAD model to minimize computational load without sacrificing accuracy, the definition of internal heat dissipation sources for active components, and surface conductance mappings between contact materials. Additionally, a mesh independence study is performed to verify that results remain stable across different mesh densities. Finally, environmental thermal testing is conducted using a thermal ambient chamber to validate the simulation results and confirm the payload's thermal resilience under realistic conditions.

This paper is structured as follows: Section 2 outlines the material properties and constitutive models used in the analysis. Section 3 details the methodology, including boundary conditions and heat flux considerations. Section 4 presents the finite thermal analysis. Section 5 provides the results and discussion, comparing simulation outcomes with experimental data. Section 6 concludes with key findings and future work recommendations.

2. Material Constitutive Model

The thermal analysis of the AlMunther payload utilized a thermomechanical model incorporating a range of materials commonly used in CubeSat payload design. The material selection aimed to represent actual components while ensuring that thermal properties such as conductivity, emissivity, density, and specific heat were accurately modeled to capture the system's real-world thermal response.

The thermal properties of these materials—such as density, specific heat capacity, thermal conductivity, and emissivity—were extracted from reputable literature sources and online databases. Table 1 summarizes selected thermal properties of key materials used in the model. To enhance analysis accuracy and simulate a real-case scenario, the AlMunther payload was integrated with a 3U structure. Figure 1 shows the assembled thermomechanical model with the materials assigned to each component in the model.

Table 1. Material properties of the different materials used in the thermomechanical model

Material	Thermal Conductivity (W/m.K)	Specific Heat (kJ/kg.K)	Density (kg/m^3)	Emissivity
FR4 [4], [5]	0.29	1.15	1850	0.8
Aluminum 6061-T6 [6], [7]	167	0.896	2700	0.039
Optical Glass [8], [9], [10]	0.95	0.753	4200	0.88
AISI 304 [11], [12]	16.2	0.5	8000	0.7
GaAs [9], [13]	46	0.33	5320	0.85
ABS Plastic [14]	0.171	1.6	1070	0.92
Black Glass-Filled Polyester [15]	0.609	1.16	1860	0.95
Brass [16], [17]	220	0.38	8890	0.8
Silicon [18]	1.05	0.785	2329	0.45

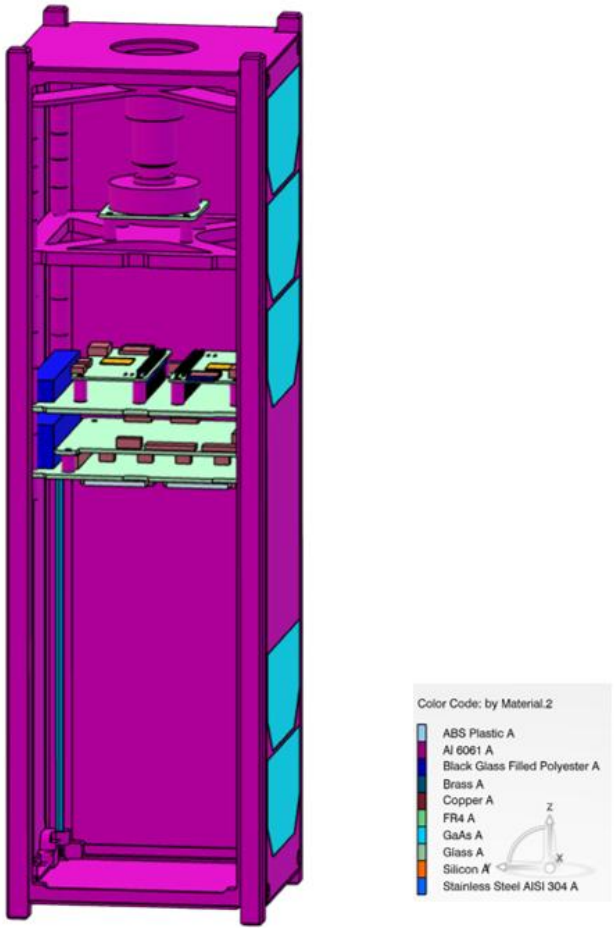

Fig. 1. The thermomechanical mode with materials colour code

3. Methodology

The analysis starts with creating a reduced model and then inputting a mesh configuration and size. The methodology will differ depending on the analysis type (i.e., transient or steady state). For steady-state hot case and transient analyses, the internal heat dissipation is defined in contrast to steady state cold case in which only Earth infrared radiation was the input. Then, surface conductance properties are defined and assigned to relevant surface contacts. The cold case steady state considers constant heat flux from Earth infrared radiation. The hot case steady state considers Earth infrared radiation, Sun radiation, and Albedo. Transient state considers variable heat flux obtained from an orbit simulation. At last, the radiation of the components to the ambient temperature or enclosure were defined. Finally, the simulation is set to run, results are obtained, and convergence analysis is conducted by setting finer meshes to the assembly. A flowchart of the methodology is presented in Figure 2.

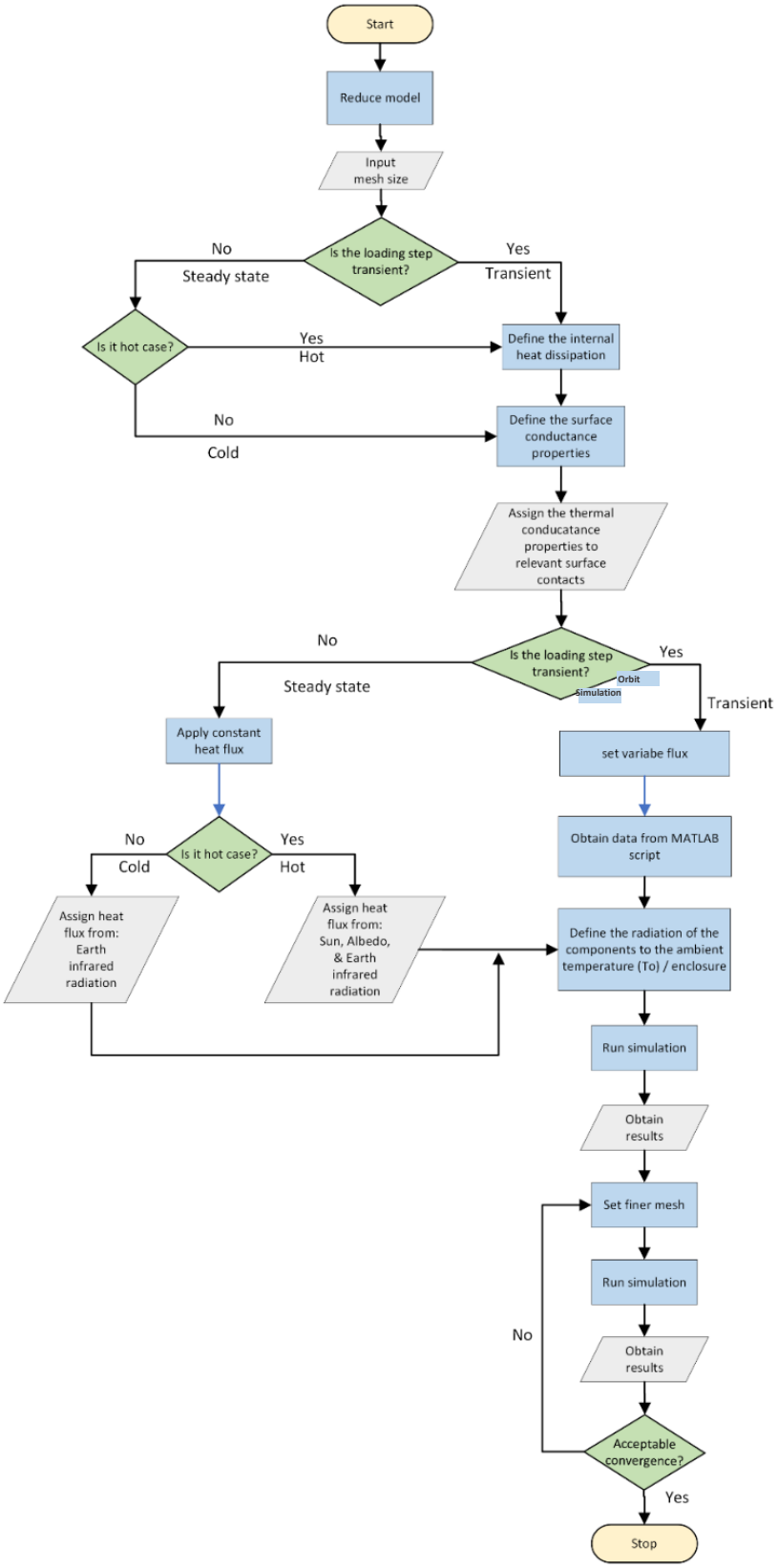

Fig. 2. Methodology flowchart followed in this work

3.1 Model Reduction

Generating a simplified Computer-Aided Design (CAD) model from the detailed CAD is the first step in conducting the thermal simulation. During the conversion, the volume is kept constant to ensure simulation accuracy. The mechanical interface remains unchanged, and no reduction was applied for the analysis. Figures 3–4 present a comparison between some components of the AlMunther payload in both simplified and detailed models. Figure 5 compares the fully assembled AlMunther payload in its detailed and simplified CAD versions. Figure 6 shows the complete assembly of the payload with the 3U CubeSat structure.

(a) Detailed CAD model (b) Simplified CAD model

Fig. 3. Comparison between the detailed and simplified CAD models for component A

(b) Simplified CAD model

(a) Detailed CAD model

Fig. 4. Comparison between the detailed and simplified CAD models for component B

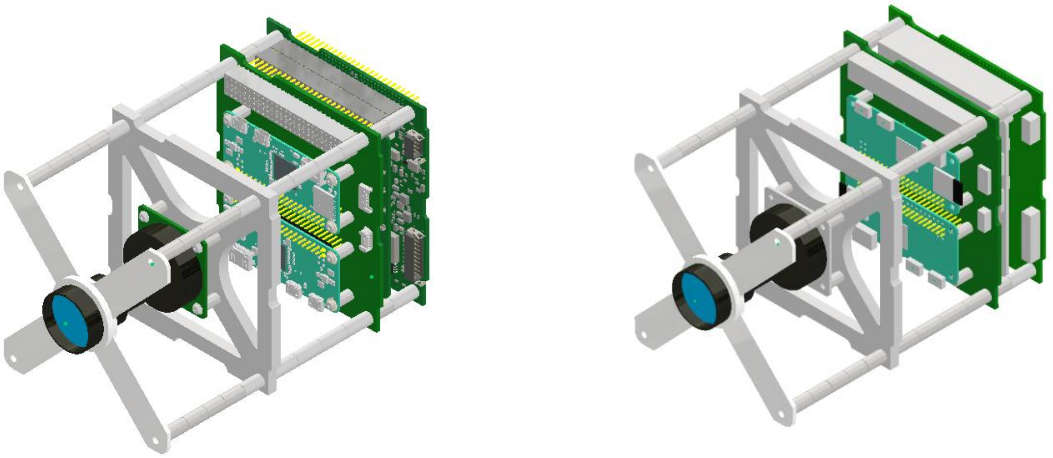

(a) Detailed CAD model (b) Simplified CAD model

Fig. 5. Comparison between the detailed and simplified CAD models of the AlMunther payload assembly

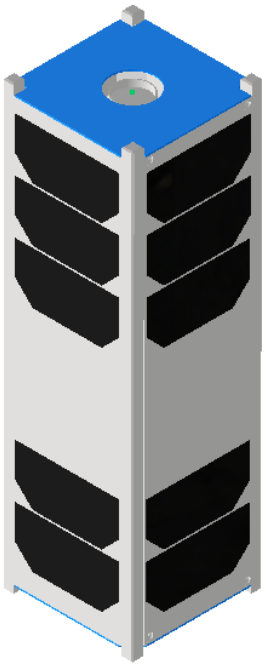

Fig. 6. Integration of the AlMunther payload in a generic 3U CubeSat structure

4. Finite element analysis

Due to the presence of a payload with multiple components, it was necessary to ensure overall thermal reliability through FEA. The analysis involved studying the temperature behavior in two thermal cases: steady state and transient state for three scenarios, namely worst case steady state hot scenario, worst case steady state cold scenario, and transient case.

There are certain parameters that were fixed in the scenarios such as the solar flux, albedo factor, the Earth IR, ambient temperature (space temperature), and the initial temperature. The worst-case hot scenario involved all the mentioned parameters, while the cold case worst case scenario involved the Earth IR only and the initial temperature. Table 2 shows the values of the fixed parameters and in which simulations they were used.

Table 2. Fixed parameters used in the thermal simulations

Parameter	Value	Simulation

Solar Flux	1367 W/m^2	Hot case
Albedo Factor	0.26	Hot case
Earth IR	257 W/m^2	Hot and cold cases
Ambient temperature	3.15K	Hot and cold cases
Initial temperature	283K	Hot and cold cases

4.1 Steady State Hot Case Simulation

The operational heat dissipation is enabled in the hot analysis case. This case corresponds to a considerable amount of exposure to Solar, Albedo, and Earth IR sources. Figure 7 shows the illustration of this case.

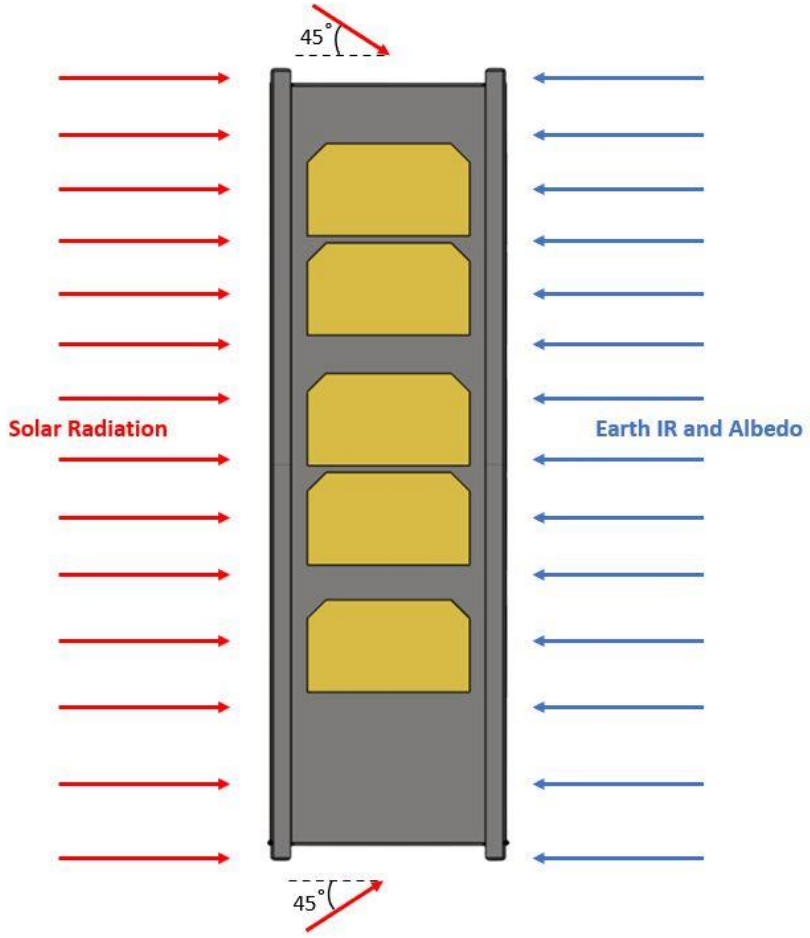

Fig. 7. Hot case loading scenario

4.2 Steady State Cold Case Simulation

The cold non-operational case can also be considered the worst-case scenario where the payloads are non-functional and maintain non-operational temperature limits. Figure 8 shows the illustration of this case.

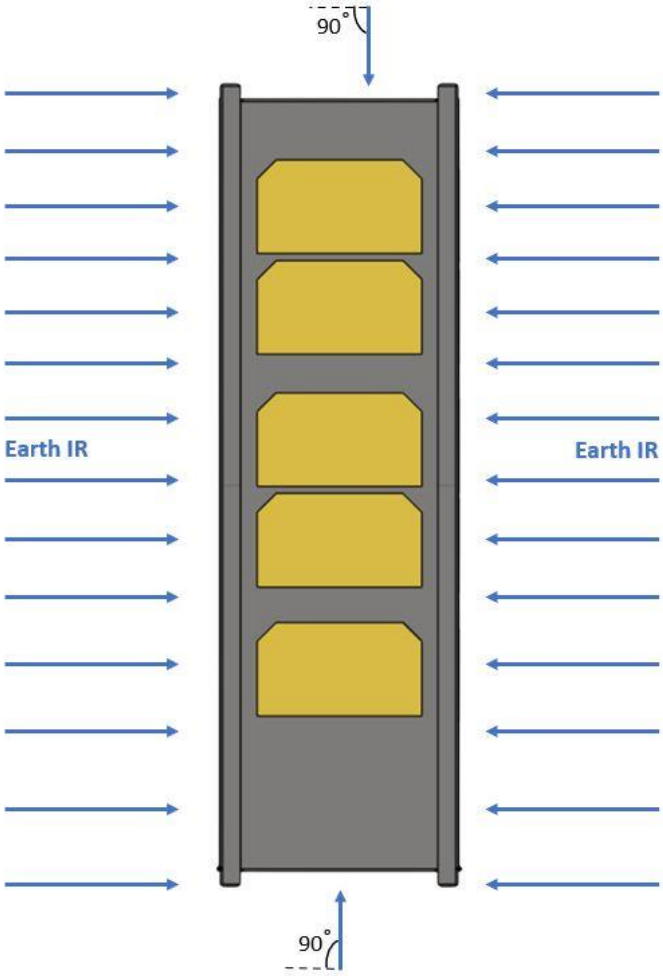

Fig. 8. Cold case loading scenario

4.3 Transient Simulation

For the transient analysis, the thermal load is considered variable and its changing based on the location of the satellite in orbit and the amount of heat incident on the satellite's surfaces. The transient load was calculated from an orbit simulation. Table 3 shows the input parameters used for the orbit simulation. Figures 9-11 shows the heat flux incident on the 3U CubeSat structure for all axes.

Table 3. The input parameters of the orbit simulation

Parameter	Value	Unit
Inclination angle	97.59	Degree
RAAN angle	121.4	Degree
Initial altitude	550	km
Rate of drop of altitude	0.25	km/day
Vernal Equinox	20 Mar 2024	-
Epoch Date	01 Feb 2024	-
Date of interest	27 Feb 2024	-
Number of days	360	-
Type of Attitude	Nadir-pointing	-
Roll	0	Degree
Pitch	0	Degree
Yaw	0	Degree

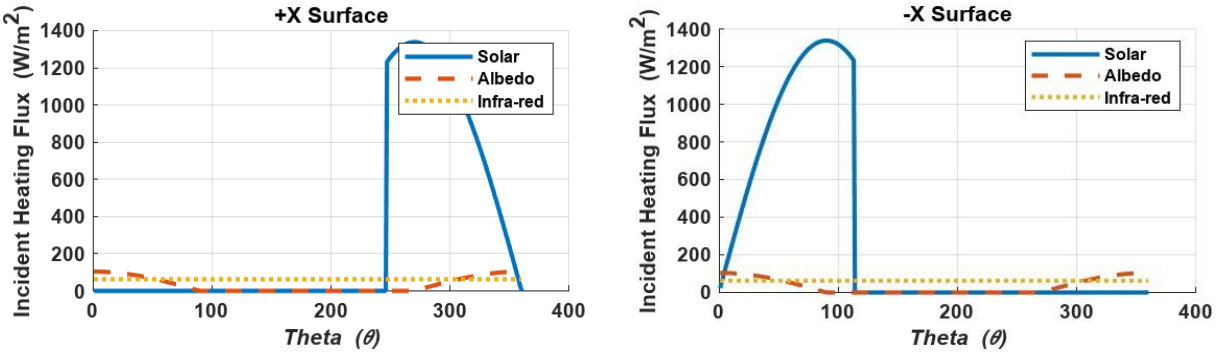

(a) Heat flux incident on the +X surface (b) Heat flux incident on the -X surface

Fig. 9. Heat flux incident for the X-axis of the 3U CubeSat

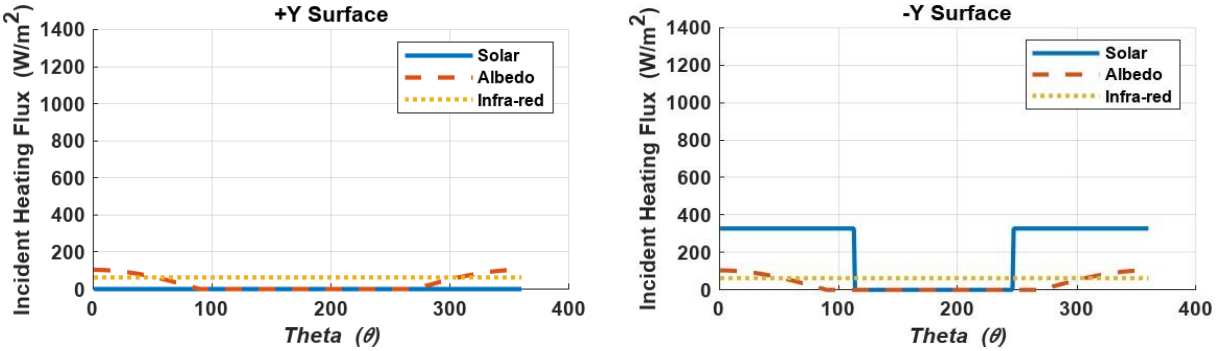

(a) Heat flux incident on the +Y surface (b) Heat flux incident on the -Y surface

Fig. 10. Heat flux incident for the Y-axis of the 3U CubeSat

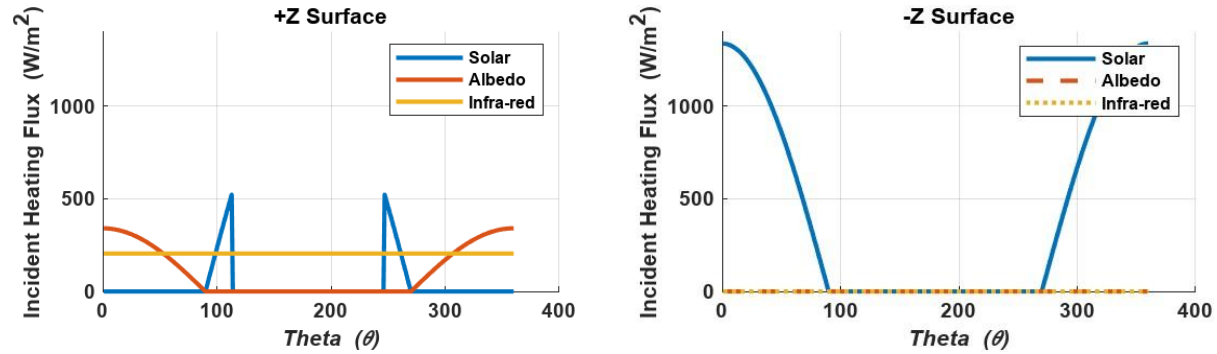

(a) Heat flux incident on the +Z surface (b) Heat flux incident on the -Z surface

Fig. 11. Heat flux incident for the Z-axis of the 3U CubeSat

5. Results and discussion

The results are presented for the three cases, namely the steady state hot case, the steady state cold case and the transient case. The FEA results show that the maximum temperature reached by the AlMunther payload under the steady state hot scenario was 322 K (49 C) where it occurred at the spacers between the camera mount and lens mount. On the other hand, the lowest temperature reached under the steady state cold scenario was 277 K (4 C) where it occurred at the camera lens glass. Figure 12 and Figure 13 show the results of the simulation for the hot case and the cold case, respectively.

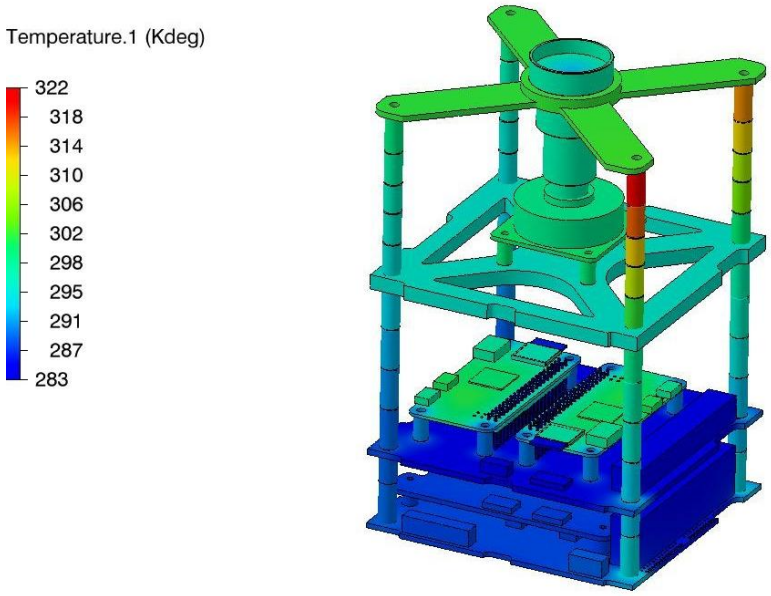

Fig. 12. Results of the steady state hot case for the AlMunther payload

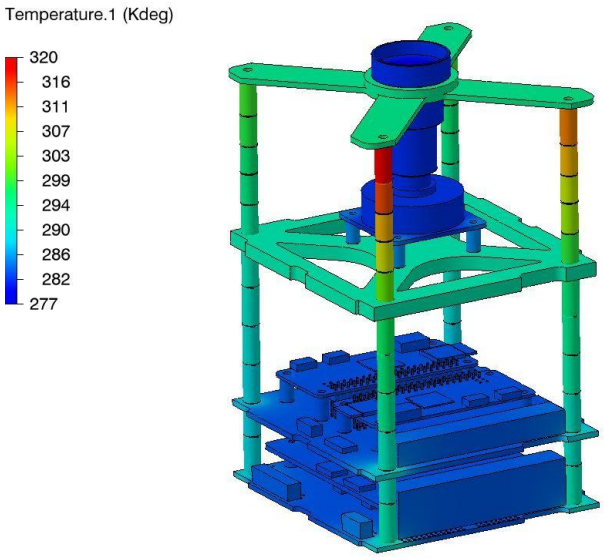

Fig. 13. Results of the steady state cold case for the AlMunther payload

In the transient case, the maximum temperature reached was 302 K (29 C) where it occurred at the processing units. Figure 14 shows the results of the transient simulation. Based on the results of all the conducted analyses, it can be concluded that all the components are within the operating temperatures obtained from the components datasheets.

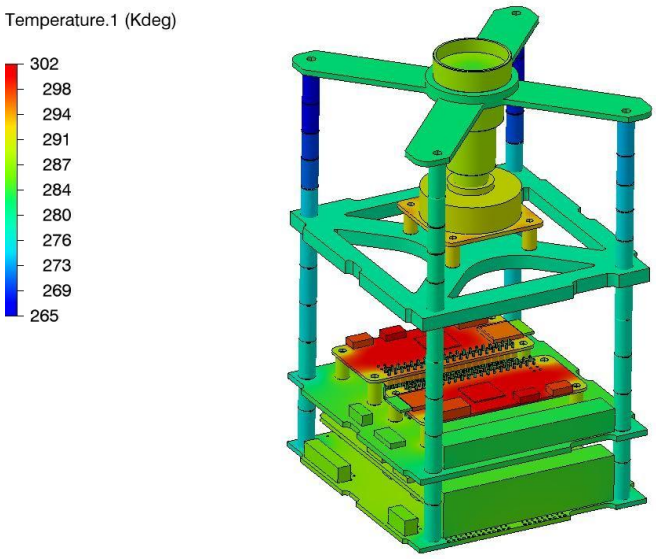

Fig. 14. Results of the transient case for the AlMunther payload

6. Conclusions

The thermal analysis of the AlMunther payload has demonstrated that all components remain within their acceptable operational temperature ranges under worst-case hot and cold conditions. Steady-state analyses indicated that the maximum temperature reached under hot conditions was 322 K (49°C) at the camera mount spacers, while the lowest temperature under cold conditions was 277 K (4°C) at the camera lens glass. Transient analysis further validated the payload's ability to withstand thermal fluctuations throughout an orbit, with a peak temperature of 302 K (29°C) observed at the Raspberry Pi modules.

The addition of an aluminum thermal shield to the payload had minimal impact on overall temperature distribution but significantly improved radiation shielding for sensitive electronics. The findings confirm that the proposed thermal control strategy effectively mitigates thermal risks and ensures reliable operation in space.

Future work will focus on refining the thermal model by incorporating additional environmental factors, such as spacecraft self-heating and component aging effects. Further validation through hardware-in-the-loop testing in a space-like thermal vacuum chamber will also be pursued to enhance the robustness of the thermal design.

References

[1] M. A. Gilmore, Spacecraft Thermal Control Handbook, Volume I: Fundamental Technologies, 2nd ed., El Segundo, CA: The Aerospace Press, 2002.
[2] ECSS-E-HB-31-03A, "Thermal Analysis Handbook," European Cooperation for Space Standardization, 2011.
[3] C. D. Macdonald et al., "Thermal Control of CubeSats: Passive and Active Strategies," Acta Astronautica, vol. 115, pp. 247–255, 2015, doi: 10.1016/j.actaastro.2015.06.007.
[4] M. Bulut, "Thermal Design, Analysis, and Testing of the First Turkish 3U Communication CubeSat in Low Earth Orbit," J. Therm. Anal. Calorim., Feb. 2021, doi: https://doi.org/10.1007/s10973-021-10566-z.
[5] "FR4 Thermal Properties to Consider During Design," NW Engineering, [Online]. Available: https://www.nwengineeringllc.com/article/fr4-thermal-properties-to-consider-during-design.php
[6] "AL 6061-T6 Aluminum Alloy Properties," The World Material, May 24, 2020. [Online]. Available: https://www.theworldmaterial.com/al-6061-t6-aluminum-alloy/
[7] San Jose State University, [Online]. Available: https://www.sjsu.edu/ae/docs/project-thesis/Justin.Lai-F15.pdf
[8] "Glass: Density, heat capacity, thermal conductivity," Material Properties, Jun. 2021. [Online]. Available: https://material-properties.org/glass-density-heat-capacity-thermal-conductivity
[9] "TIE-31 Mechanical and Thermal Properties of Optical Glass," University of Arizona. [Online]. Available: https://wp.optics.arizona.edu/optomech/wp-content/uploads/sites/53/2016/10/tie-31_mechanical_and_thermal_properties_of_optical_glass_us.pdf

[10] "Table of Total Emissivity," Omega Engineering. [Online]. Available: https://assets.omega.com/pdf/tables_and_graphs/emissivity-table.pdf
[11] "Emissivity of Various Surfaces," Transmetra. [Online]. Available: https://www.transmetra.ch/images/transmetra_pdf/publikationen_literatur/pyrometrie-thermografie/emissivity_table.pdf
[12] "AISI 304 Grade Stainless Steel Properties," The World Material, Jul. 31, 2020. [Online]. Available: https://www.theworldmaterial.com/type-304-grade-stainless-steel/
[13] "Gallium Arsenide (GaAs)," Janis Research Company. [Online]. Available: https://www.janis.com/docs/default-source/default-document-library/gallium-arsenide-gaas-transmission-curve-datasheet.pdf
[14] "Overview of Materials for Acrylonitrile Butadiene Styrene (ABS)," MatWeb. [Online]. Available: https://www.matweb.com/search/DataSheet.aspx?MatGUID=eb7a78f5948d481c9493a67f0d089646
[15] "Overview of Materials for Thermoset Polyester Glass Filled BMC," MatWeb. [Online]. Available: https://www.matweb.com/search/datasheet.aspx?matguid=c9a9ff9a99ca46df81c2e21178e0f2ed
[16] "Brass," MatWeb. [Online]. Available: https://www.matweb.com/search/DataSheet.aspx?MatGUID=d3bd4617903543ada92f4c101c2a20e5
[17] "Copper Properties," MatWeb. [Online]. Available: https://www.matweb.com/search/DataSheet.aspx?MatGUID=9aebe83845c04c1db5126fada6f76f7e
[18] "Overview of Materials for Silicone Rubber," MatWeb. [Online]. Available: https://www.matweb.com/search/DataSheet.aspx?MatGUID=cbe7a469897a47eda563816c86a73520